

## Microspacecraft Platform with Bipropellant Propulsion System and 3-Axis Stabilization for Missions in Earth Orbit and Beyond LEO

*P. Eckart<sup>1</sup>, S. Angelucci<sup>1, \*</sup>, L. Appolloni<sup>1, \*</sup>, H. Baier<sup>2</sup>, M. Canales<sup>1</sup>, A. da Silva-Curiel<sup>6</sup>, E. Freidl<sup>4</sup>, E. Igenbergs<sup>1</sup>, M. Kesselmann<sup>5</sup>, T. Neff<sup>1</sup>, K. Pauly<sup>1, \*\*</sup>, T. Pühlhofer<sup>2</sup>, F. Schlerka<sup>1</sup>, W. Seefelder<sup>1</sup>, L. Tarabini<sup>1</sup>, A. Straub<sup>3</sup>, S. Ullmann<sup>1</sup>*

*<sup>1</sup>Division of Astronautics, Technische Universität München, Germany  
phone +49-89-289-16016; fax +49-89-289-16004; email p.eckart@lrt.mw.tum.de*

*<sup>2</sup>Chair of Lightweight Structures, Technische Universität München, Germany*

*<sup>3</sup>Universität der Bundeswehr (German Forces), Neubiberg, Germany*

*<sup>4</sup>Daimler-Chrysler Aerospace, Ottobrunn, Germany*

*<sup>5</sup>OHB System GmbH, Bremen, Germany*

*<sup>6</sup>Surrey Satellite Technology Ltd., Guildford, UK*

*\*Now: ESA-ESTEC, Noordwijk, The Netherlands*

*\*\*Currently: NASA, Johnson Space Center, Houston, TX*

### Abstract

This paper presents a low-cost microspacecraft platform concept for missions which require high  $\Delta$ -v capabilities of up to about 1,500 m/s, using auxiliary launch opportunities, e.g., from the Ariane 5 ASAP. The proposed concept is extremely flexible and can be adapted to specific mission requirements, thus permitting low-cost missions to Earth orbit, as well as to the Moon, Mars, and selected asteroids. A particular focus of this paper is on the modularity of the proposed concept, including the bipropellant propulsion system needed to provide the required  $\Delta$ -v, the lightweight structural concept, and the 3-axis attitude determination and control system (ADCS), as well as the available P/L masses and the most important spacecraft characteristics and constraints.

The proposed microspacecraft platform is derived from the LunarSat concept, which has

been developed by a team led by the Technische Universität München, Germany, and Surrey Satellite Technology Ltd., UK. Consequently, the LunarSat spacecraft and mission are presented as an example of the proposed concept.

### Introduction

Microsatellites have recently become a viable alternative for a variety of applications. This is due to new mission concepts, as well as major advances in microelectronics and increasing availability of commercial off-the-shelf (COTS) components. Although a lot of missions will continue to require large spacecraft solutions, low-cost satellite solutions are becoming increasingly attractive in the light of decreasing space budgets. When compared to conventional development procedures, small satellite projects are mainly characterized by rapid development scales, comparatively low spacecraft development cost, and the possibility to use low-cost, auxiliary launch options.

As indicated, the concept presented here is derived from the LunarSat concept. LunarSat shall be sent into an orbit around the Moon to perform scientific investigations concerning the lunar environment and its characteristics. It shall be launched as an auxiliary payload on an Ariane 5 ASAP platform, shall have a mass of less than 120 kg in GTO, and shall orbit the Moon on a highly elliptical polar orbit with its perilune above the lunar south pole area.

### **Mission Design**

A microsatellite, i.e., a spacecraft with a mass of only about 100 kg can have a maximum  $\Delta$ -v capability of about 1500 m/s, using conventional propulsion technology. Therefore, their scope of missions from GTO is limited to:

- Selected Earth orbits
- Lagrangian points of the Earth-Moon system
- Lunar orbit
- Mars fly-by
- Near-Earth object fly-by

As an example, the lunar orbit mission case is presented below. Preliminary analyses for a Mars missions and Lagrangian point missions have also been conducted.

There are several methods of transfer from GTO to lunar orbit. The exact conditions of the GTO in space and time will determine which of these options will be the most efficient one. Maximum trans-lunar injection (TLI) maneuver efficiency is achieved by a coplanar tangential thrust. In this case, the lunar transfer orbit (LTO) is obtained by a perigee maneuver raising the GTO apogee to the distance of the Moon. This means that GTO and LTO need to have nearly the same orbital orientation. Since the transfer strategy to be developed must

provide permanent transfer opportunities from GTO, a solution has to be found that achieves an inclination adjustment between the Earth equator and the orbit of the Moon at a minimum fuel consumption.

Since the mass of the Moon is only about 1/80th the mass of the Earth, the Earth-Moon system comes close to being a double planet. Thus, both the Earth and the Moon revolve about their common center of mass, which is located about 4,671 km from the center of the Earth. The motion of the Earth-Moon system results from a complex balance and counterbalance of gravitational forces, mainly of the Sun, Earth and the Moon. The orbit of the Moon, rotating about the Earth-Moon center of mass, has the following characteristics:

- Sidereal Period: 27.32166 days
- Synodic Period: 29.53059 days
- Mean Apogee Radius: 405,508 km
- Mean Perigee Radius: 363,300 km
- Mean Semi-Major Axis: 384,404 km
- Mean Eccentricity: 0.054900573
- Mean Inclination w.r.t. Ecliptic: 5°8'43''

The line of nodes rotates westward with respect to the ecliptic as the fundamental plane, making one complete revolution in 18.6 years. The line of apsides rotates in the direction of the Moon's orbital motion, causing the argument of perigee to change by 360° in about 8.9 years. The inclination of the Moon's orbit with respect to the Earth's equatorial plane is subject to the rotation of its nodal line. When the Moon's ascending node coincides with the vernal equinox direction, the inclination of the Moon's orbit to the equator is at its maximum, being the sum of 5°8' and 23°27' or 28°35'. When the descending node is at the vernal equinox, the inclination of the Moon's orbit to the equator is at its minimum, being the difference of 23°27' and 5°8' or 18°19'. Thus, the inclination relative to the equator varies between 18°19' and 28°35' with a period 18.6 years.

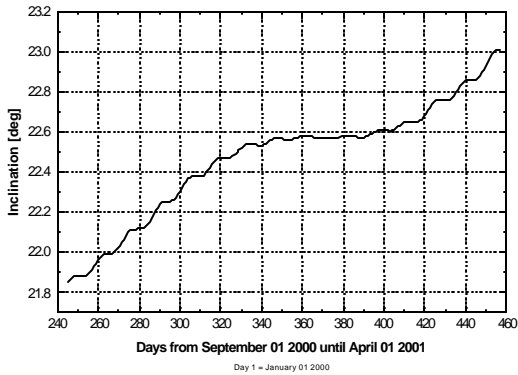


Figure 1: Inclination of the Moon's Orbit

Figure 1 shows the inclination of the Moon's orbit relative to the equatorial plane within the probable LunarSat launch period. The right ascension of the ascending node of the Moon's orbit in the J2000.0 reference frame within the probable LunarSat launch period is plotted in Figure 2. The x axis is parallel to the mean Earth equator of epoch J2000.0.

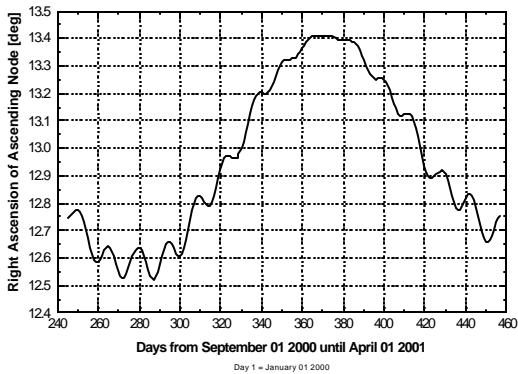


Figure 2 Right Ascension of Ascending Node of the Moon's Orbit

In the following different transfer strategies that have been investigated in order to meet the objectives of the LunarSat mission are described.

### Short Transfer Trajectory

A perigee maneuver injects the spacecraft into a LTO with an apogee distance close to the Moon's distance. Due to the low declination

angle of the Moon at encounter, only a small inclination change maneuver is required, which can be applied as a LTO mid-course maneuver with an acceptable fuel consumption. In a two-body consideration, the mid-course maneuver must take place just before crossing the Moon's sphere of influence. A third impulsive kick is required to enter the final orbit.

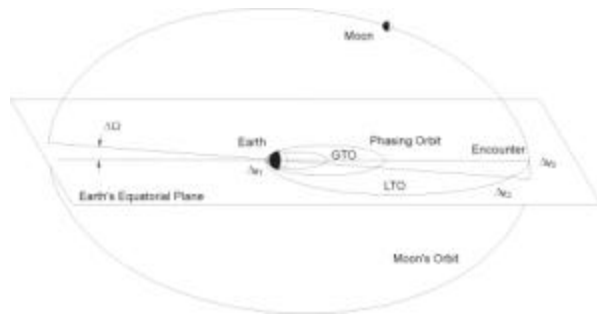


Figure 3: Short Transfer Strategy

### Long Transfer Trajectory

In the case, the bi-elliptic orbit is chosen, the spacecraft is injected into a very highly eccentric LTO with an apogee distance of about 1 million km.  $\Delta v_2$  is accomplished to enter the incoming leg of the second transfer ellipse and to adjust the inclination simultaneously. This maneuver is applied at the apogee of the transfer ellipses at a distance of about 1 million km away from Earth, such that the velocity vector is very small. Since the inclination change maneuver is related to the actual orbital velocity when the maneuver is performed, this strategy considerably reduces the cost of an out-of-plane maneuver. Again, a third impulsive kick is required to enter the final orbit.

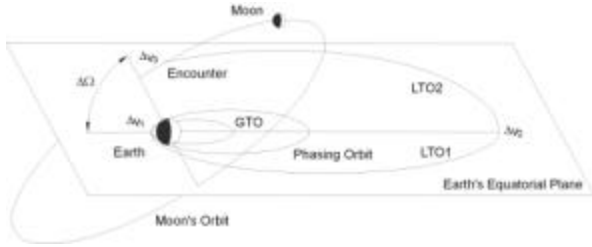


Figure 4: Long Transfer Strategy

In Figure 4 the situation for a nodal difference of  $\Delta\Omega=90^\circ$  is illustrated.

#### Transfer Orbit using a Lunar Flyby

In order to have the possibility to perform small adjustments on the lunar arrival conditions, a single lunar flyby is employed prior to lunar orbit injection. The apogee manoeuvre has to be applied to aim at the Moon. The flyby at the Moon enables the rotation of the arrival orbit's plane, so that the optimum conditions at the lunar orbit injection can be achieved.

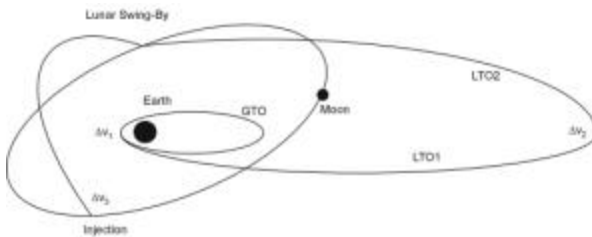


Figure 5: Transfer using a single Lunar Flyby

#### Weak Stability Boundary Transfer

The WSB transfer orbit crosses through a region 1.4 – 1.5 million km away from Earth which is referred to as the Earth-Sun Weak Stability Boundary (WSB). Under certain circumstances, passing by this region provides the possibility to make use of strong solar perturbations in order to return a spacecraft to the orbit of the Moon without the requirement of major thrust maneuvers. Reaching the vicinity of the Moon, the effects of the Earth-Moon WSB region can be employed to obtain a

ballistic capture at the Moon. The result is an unstable high-elliptical lunar orbit. In the optimum case a lunar orbit can be reached applying a single GTO perigee maneuver. A small thrust maneuver is required to stabilize or to enter a nominal operational orbit around the Moon. Figure 6 shows a WSB transfer crossing through the Earth-Sun and Earth-Moon fuzzy boundary regions.

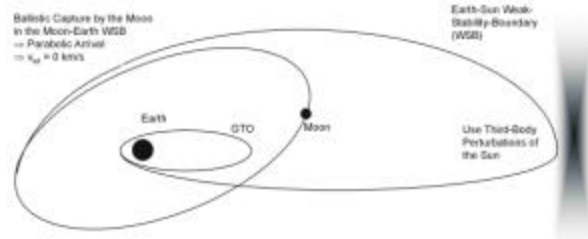


Figure 6: Weak Stability Boundary Transfer

#### Results for Hohmann and Bi-elliptic Transfer

In the case of the Hohmann and the bi-elliptic transfer the declination of the Moon at encounter was given to be the criterion to decide on the transfer strategy. This angle is directly related to the angular difference between the GTO's line of nodes and the nodal line of the Moon's orbit. The strategy, that is actually used is referred to (Ref.3):

- Long Transfer:  $29 \text{ deg} < \Delta \text{Node} < 134 \text{ deg}$   
 $207 \text{ deg} < \Delta \text{Node} < 315 \text{ deg}$
- Short Transfer:  $134 \text{ deg} \leq \Delta \text{Node} \leq 207 \text{ deg}$   
 $315 \text{ deg} \leq \Delta \text{Node} \leq 29 \text{ deg}$

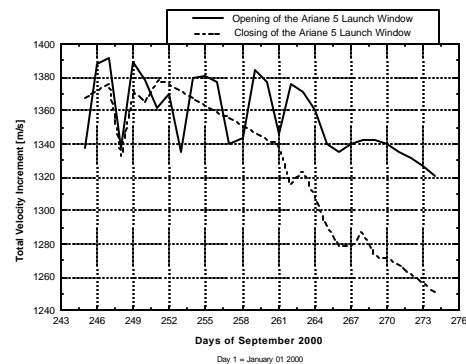


Figure 7: Total DV for September 2000

The total velocity requirement for September 2000 for the Hohmann and bi-elliptic transfer are shown in Figure 7. The maximum  $\Delta v$ -requirement to reach a six hour lunar orbit is close to 1390 m/s.

### Results for the WSB Transfer

The WSB transfer to the Moon has been investigated entering a four hour lunar orbit. The difference in  $\Delta v$  between a six hour and a four hour lunar orbit is close to 100 m/s. For the case where only solar perturbations at the apogee have been taken into account, the obtained total velocity requirement for the launch period April 2001 is printed in Figure 8. The values are given for the opening and the closing of the Ariane 5 mid-night launch window.

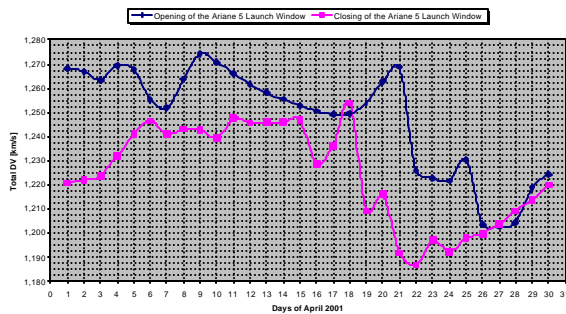


Figure 8: Total Velocity Requirement April 2001

These results clearly show that only using solar perturbations at the apogee of the transfer orbit considerably contributes to  $\Delta v$  reductions. The calculated strategy still enters lunar orbit by a high thrust capture manoeuvre on a hyperbolic arrival trajectory. Therefore, a further saving in the total velocity requirement is expected using also the effects of the Earth-Moon WSB region. The following figures show a solution for a Weak Stability Boundary transfer, using the Earth-Sun as well as the Earth-Moon fuzzy

boundary region. A ballistic capture at the Moon is achieved after a multiple flyby. The flybys occur due to the chaotic dynamics of the spacecraft within the Earth-Moon WSB region. In the given solution only a GTO perigee burn is applied to enter lunar orbit.

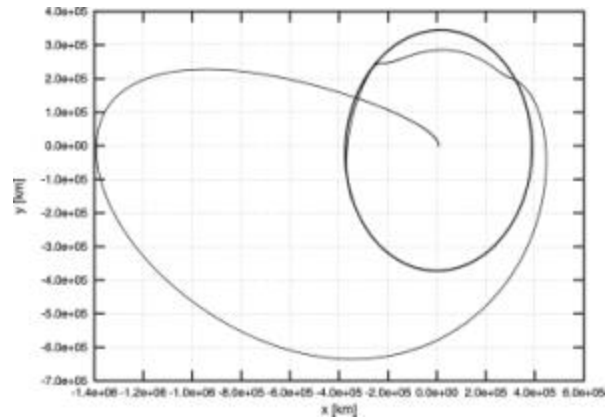


Figure 9: X-Y View of a WSB Transfer

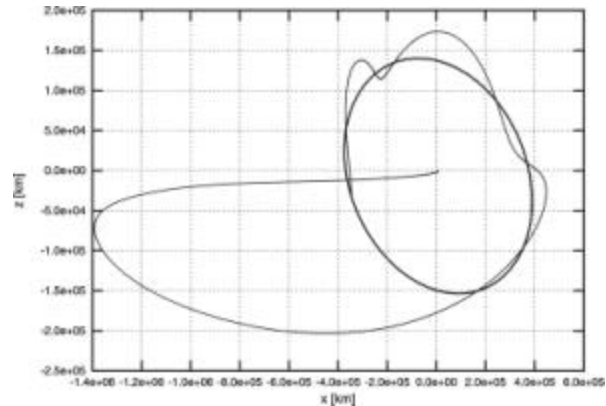


Figure 10: X-Z View of a WSB Transfer

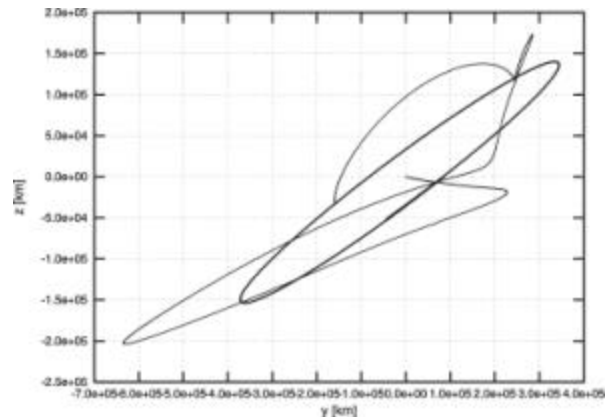


Figure 11: Y-Z View of a WSB Transfer

The minimum  $\Delta v$ -requirement to reach a four hour lunar orbit for the given launch period is close to

1130 m/s. The average time of flight ranges between 70 and 90 days. The classical transfer strategies have shown a minimum of 1250 m/s considering a six hour lunar orbit. Therefore, potential savings up to the order of 250 m/s in propellant can be obtained using a WSB transfer strategy. Also trajectories were found, that fly by the Moon prior to the apogee of the transfer orbit. They have been designed to further reduce the total velocity requirement by lowering the thrust manoeuvre at the GTO perigee, required to accelerate the spacecraft toward apogee.

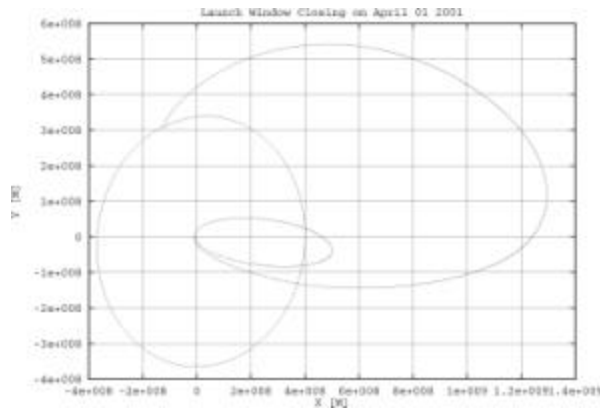


Figure 12: X-Y View of a WSB-Swing-By Transfer

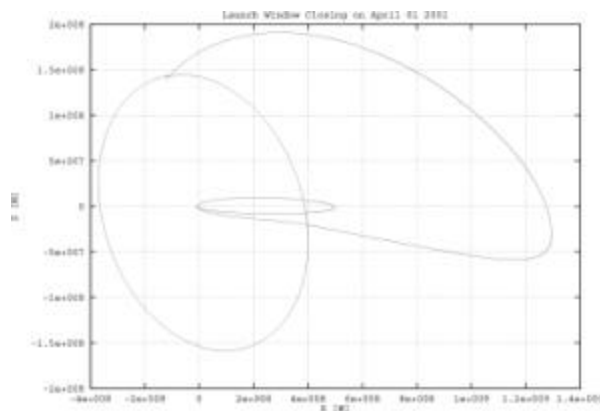


Figure 13: X-Z View of a WSB-Swing-By Transfer

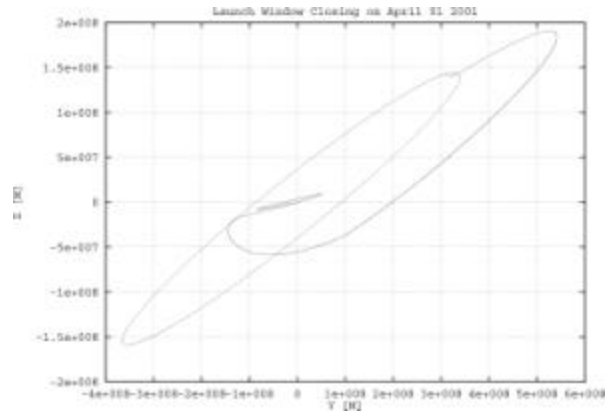


Figure 14: Y-Z View of a WSB-Swing-By Transfer

The lunar swing-by maneuver slightly lowers the velocity requirement to inject into the LTO. But it does not contribute considerably to a reduced total velocity requirement.

### Spacecraft Structure and Configuration

In the following, the design of a microspacecraft for launch on an Ariane 5 auxiliary platform (ASAP) is presented. This design is based on the work that has been conducted for LunarSat.

The maximum allowed spacecraft size and mass, as defined in the Ariane 5 ASAP user manual, are 600x600x800 mm<sup>3</sup> and 120 kg, respectively. Consequently, the main considerations in selecting a shape for such a microspacecraft are:

- Packaging considerations, i.e., to provide enough volume to contain the subsystem components and to fit within the fairing envelope.
- Structural considerations, i.e., compatibility with the payload and launch vehicle mechanical interfaces and efficient, in-line structural load paths between payload and launch-vehicle

The most important criterion for selection of the spacecraft shape is that it must be able to contain the largest packaged components. Because of the desired velocity capability of up to 1500 m/s a microspacecraft requires about 60% of its total wet mass for the propulsion system. This means that the

design process is mainly ruled by considerations regarding the required tank volume that has to fit inside the ASAP envelope. Other critical layout criteria are that at launch the spacecraft center-of-mass (C.M.) must be not more than 5 mm away from the center line (ASAP requirement), and that the structural mass has to be minimized. Several spacecraft designs have been investigated.

The proposed microspacecraft is divided into two main segments:

- Payload Bay, which contains all payload and sensors, plus TT&C and OBDH and parts of EPS subsystem of the spacecraft.
- Service Bay, which contains the main thrusters, the propellant tanks and all propulsion elements. The proposed system uses four main thrusters with a thrust level of 22N each, using NTO and hydrazine. Four 1N hydrazine thrusters are used for attitude control, along with three reaction wheels. Also situated in the service bay are the Li-ion batteries and the laser gyros.

Several configurations have been analyzed for the propulsion system, for which five tanks (two for the required fuel, two for the oxidizer and one pressure vessel) are required.

The resulting baseline design uses a symmetrical tank configuration of four propellant tanks (2+2), all mounted on the same level. The pressure tank is mounted below these four tanks, on the geometric center axis. The propellant tanks are located on the tank panel (Middle Tank Plate - MTP) of the propulsion module. This configuration is shown in figure 15.

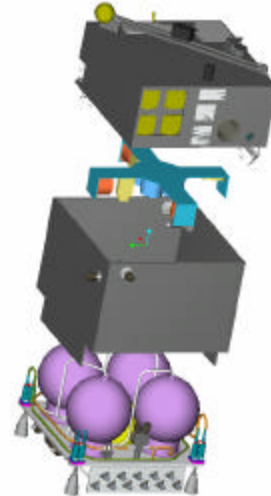


Figure 15: Baseline Spacecraft Configuration

## Propulsion System Design

As indicated, the proposed microspacecraft shall have a total  $\Delta$ -v capability of about 1500 m/s, using a dual-mode propulsion system. This means that bi-propellant main engines and monopropellant attitude thrusters will use the same fuel: hydrazine. Due to constraints in size and mass of the spacecraft, a propellant combination with a high energy density had to be chosen.

### Propulsion System Design Baseline

The proposed baseline design of the propulsion system (see figure 16) is composed of:

- Four 22 N main engines using pure hydrazine ( $N_2H_4$ ) as fuel and nitrogen-tetroxide ( $N_2O_4$ ) as oxidizer, with a specific impulse  $I_{sp}=289s$  and a mixture ratio  $\phi = 1.164$
- Four mono-propellant (hydrazine) 1N attitude thrusters
- A tank-pressure-feed system with:
  - ♦ *Propellant storage:* (propellant tank structure propellant expulsion assembly) two hydrazine tanks in series as well as two NTO tanks in series with the same diameter, each tank containing a passive

propellant management device (surface tension) for fuel expulsion in 0g, with a maximum fill rate of 94% and 1% residual (propellant flow schematic)

- ♦ *Tank pressurization*: one helium high pressure (177 bar) tank to ensure that the propellant tank maintains the desired pressure
- ♦ *Propellant flow control*: one pressure regulator, pyrotechnic valves, check valves, pipes, pressure transducers and filters for propellant flow control

- Temperature sensors at critical points
- Heaters

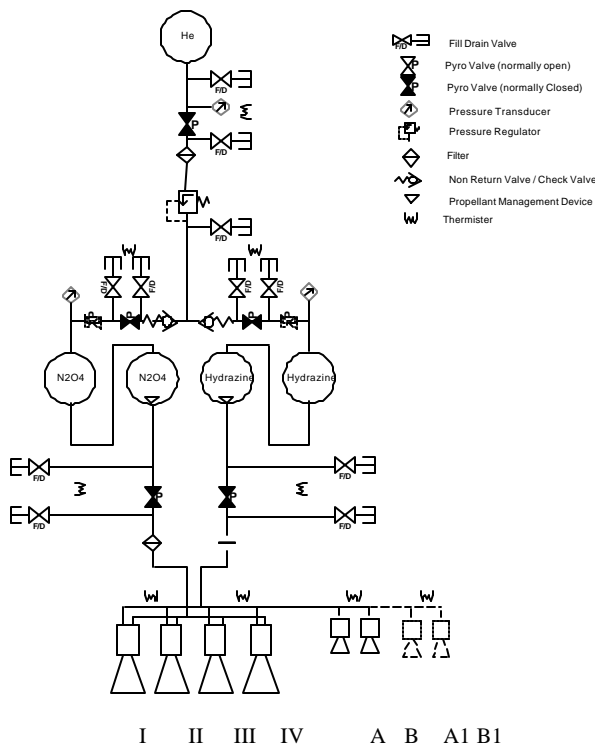


Figure 16: Design Baseline of the Propulsion System

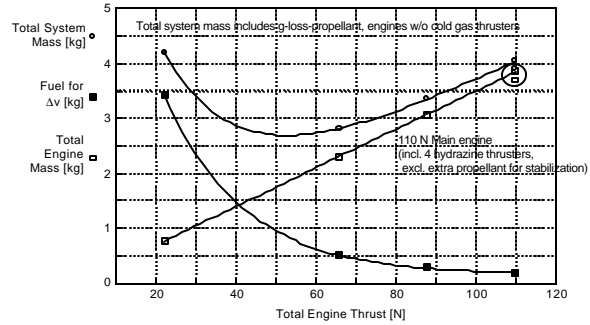


Figure 17 Gravity Losses for Injection Maneuver from GTO to LTO (1.5 Million. km Apogee Height)

After conducting a trade-off regarding the influence of thrust and main engine mass on gravity losses during the injection firings, a four engine configuration (used in pulsing mode) has been selected. Specifically; for LunarSat the injection firing from GTO into LTO was investigated as a reference because its Δv of about 565 m/s is most decisive concerning the g-losses. Figure 17 indicates the fuel requirements due to gravity losses during the burn period.

### Propulsion System Layout

The serial arrangement of hydrazine and NTO tanks offers several advantages compared to parallel tank expulsion: no active expulsion control is required and components like F/D valves and pyro-valves are much more lightweight than latch valves. On the other hand, the serial solution causes a predictable shift of the center of mass (CM) of the spacecraft during tank expulsion, which requires an active attitude control during main engine firing. In order to keep the misalignment of the CM from the spacecraft geometrical center line as small as possible, a propellant flow schematic as shown in figure 18 is used.

The propellant tanks are mounted on the tank panel (Middle Tank Plate - MTP) of the propulsion module. The mounting is performed by an egg-cup configuration, which are connected to the panels via

bolts. The helium pressurant tank is fastened on their two pole ends on the hole of the MTP with one free polar displacement fitting. All components for the pressurant control (PC) and propellant assembly (PA) are preintegrated on modules, that latter are again attached to the structure.

Main engines and attitude thrusters are already provided with a serial solenoid valve each. In case of a thruster failure the affected engine can be isolated separately by the solenoid valves. Three NC (normally closed) pyro-valves provide also positive dual isolation of the pressurant tank from the propellant tank prior to the activation of the propulsion system after separation from the ASAP-platform. NO (normally open) pyro-valves are also added to isolate pressure regulator and helium tank from the rest of the system in case of malfunction of the pressure regulator.

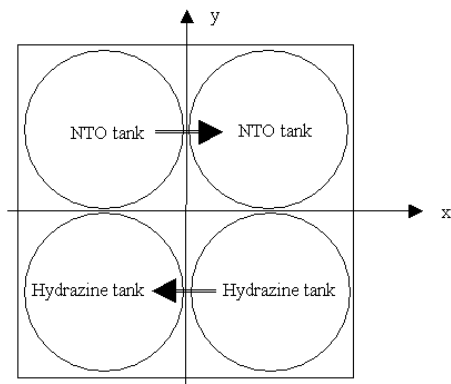


Figure 18: Propellant Flow Schematic

The tanks and fluid components are connected using either 3/8 inch or 1/4 inch, 0.028 inch wall 3Al-2.5V titanium tubing. Safety factors (Burst/MEOP) that are required to be met by the system are: Tanks  $\geq 2.0$ , components  $\geq 2.5$  and lines  $\geq 4.0$ . All designs for the flight system and GSE must satisfy MIL-STD 1522A as well as Ariespace launch vehicle requirements.

The microspacecraft propulsion system, shown in Figure 19, is comprised of two major elements, the core module with fluid tanks and the piping module.

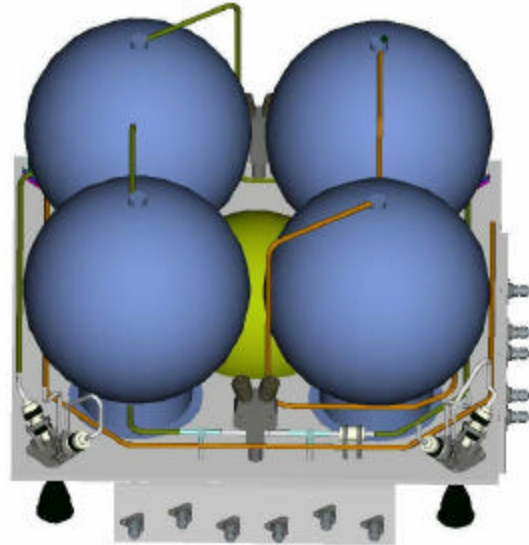


Figure 19: Middle Tank Plate with Propellant and Pressurant Tanks

The driving design aspect of the propulsion system is cost effectiveness. This goal is achieved by three means:

- Using COTS components, in order to avoid developing costs.
- Integration of the propulsion system mainly on one device to shorten assembly time and to gain a high modularity and flexibility in production.
- Establishing a modular construction system of the whole S/C for adapting the main design easily to variable mission profiles.

### Main Thruster Selection

Investigations have been conducted regarding the selection of the main thrusters. Three available main engines and various configurations have been investigated.

The main parameter of the study is the required tank diameter, i.e., the required propellant mass. The required propellant mass without any losses can be

calculated using the Tsiolkovsky equation which leads to a required propellant mass:

$$m_{prop} = m_i \left( 1 - e^{\frac{-\Delta v}{I_{sp} g_0}} \right) \quad (\text{eq. 1})$$

Additional propellant is required for orbit maintenance, losses, residuals, potential leakage and ADCS tasks. Specifically, for LunarSat the additionally required propellant mass for the ADCS and losses is composed of:

- Orbital Maintenance  
The worst case  $\Delta v$  for maintenance is 100 m/s even though 0 m/s could be in some cases possible according to the mission design.
- Desaturation  
Desaturation maneuvers require fuel in order to reset the angular speed of the reaction wheel to 0 rpm. These can be split into x- and y-axis desaturation maneuvers which can use 40 ms of thrust and z-axis desaturation maneuvers which can use 300 ms of thrust. According to calculations of the external disturbances acting on LunarSat during the entire mission lifetime, we can state a number of required desaturations around the x- and y-axes of 2 and a number of desaturation around the z-axis of 3.
- Safe Mode  
The Safe Mode comprises different maneuvers which have to be taken in account, in particular: detumble maneuvers, fuel settling maneuvers and thrusting maneuvers.  
The *detumble maneuver* occurs at the beginning of the mission and is required to stop the satellite from tumbling after release from Ariane 5. The calculation of this was roughly made through simulation where the

initial angular momentum had to be damped by thrusters and reaction wheels. The initial angular momentum were 1.04 Nms on the z-axis and 0.9362 Nms on the x- and y-axes.

The *fuel settling* maneuvers are needed before every firing in order to compact the bubbling fuel inside the tanks. To achieve this it is possible to pulse the 4 main engines for a short period of time (for example, 0.1 s). This maneuver will be repeated 5 times.

Some *thrusting maneuvers* could be used during LunarSat lifetime. For the calculation we design four 360° maneuvers, accomplished in 120 s around the x- and y-axes, 0.877 s around the z-axis (only not slanted configurations), accelerating and decelerating the spacecraft for 5% of the time.

- Firing  
The firing phases introduce a propellant consumption for ADCS purposes that can be originated by 5 different causes:
  - Direct thrust loss
  - Control of z-axis
  - g-loss
  - Oscillation
  - $I_{sp}$  loss

When we adopt a slanted configuration with the main engines, misaligned with respect to the z-axis we introduce a direct loss in thrust, given by the components of the thrust vector which does not act in the flight direction. This additionally required propellant mass is expressed as a percentage of propellant loss:

$$m_{dl} = m \cdot 100 \left( 1 - \cos \frac{\mathbf{a} \cdot \mathbf{p}}{180^\circ} \right) \quad (\text{eq. 2})$$

where

- $m_{dl}$  = required mass resulting from direct loss
- $m$  = propellant mass the direct loss is based upon
- $\alpha$  = slant angle [deg]

The control on the z-axis during the firing phases is obtained using the main engines in the case we have a pure slanted version, else with cold gas thrusters or with hydrazine thrusters. In any of these cases we have a propellant consumption which has to be taken into account. The additionally required propellant mass can be derived from simulations. An empirical formula that may be used is:

$$m_{cz} = \frac{0,104s}{0,00045} \cdot \dot{m} \quad (\text{eq. 3})$$

where

$m_{cz}$  = required propellant mass due to control on z-axis during firing

$\dot{m}$  = mass flow of the engines.

The g-loss is given by the less efficient thrust with respect to the nominally desired one. In this case the thrusting phase is prolonged, leading to loss in the effective thrust since the thrust becomes less instantaneous and covers a bigger part of an orbit. The g-loss depends on the engine performance, especially on the mass flow. As already mentioned above, the g-loss is referenced on the first maneuver.

The oscillation is meant to explain the losses coming from the fact that, due to control algorithms, the microspacecraft is not following a straight path but is describing a serpentine line. It can be given as:

$$m_{osc} = m_{req, \Delta v=1300m/s} \left( 1 - \cos \frac{\mathbf{b} \cdot \mathbf{p}}{180^\circ} \right) \quad (\text{eq. 4})$$

where

$m_{osc}$  = additional consumed propellant mass due to oscillation

$m_{req, \Delta v=1400m/s}$  = propellant mass resulting from rocket equation

$\beta$  = oscillation angle [deg]

The  $I_{sp}$  losses result from the control algorithm which requires the engines to be continuously off-pulsed. This leads to a worse use of the thrusters due to a longer time spent into thrust transitories. In the end, a lower  $I_{sp}$  performance is obtained and a bigger quantity of propellant is needed in order to accomplish the planned firing maneuvers.

In order to assess the propellant consumption correctly, it is necessary to keep in mind that whenever we have a slanted configuration of the main engines, the direct thrust loss affects the orbital maintenance, the safe mode and the desaturations as well. It was noticed that in case of a slanted version, by increasing the slant angle, the controllability of the spacecraft is increased, but also the propellant losses are increased. These losses can actually be partially saved by not using the attitude thrusters around the z-axis. Nevertheless, any slant configuration requires more complex algorithms and particular attention to the mounting accuracy.

An essential characteristic of the microspacecraft propulsion system is its wet mass which is composed of the sum of all single propulsion system component masses, their mechanical and electrical interfaces and the total required propellant mass. Masses of all components and required propellant tanks (tank with the maximum available diameter which will fit inside the envelope) are listed in the table 1.

The calculations of all potential options lead to the result that all three configurations are feasible.

Table 1: Propulsion System Mass Breakdown

| Propulsion System Components |         |        |           |                 |
|------------------------------|---------|--------|-----------|-----------------|
| Item                         | Comment | Number | Mass (kg) | Total Mass (kg) |
| <b>Feed System Component</b> |         |        |           |                 |
| Pressure Regulator           |         | 1      | 1.2       | 1.2             |
| Pressure Transducer          | LP      | 2      | 0.17      | 0.34            |
| Fill/Drain Valves            | HP      | 1      | 0.17      | 0.17            |
|                              | LP      | 9      | 0.07      | 0.63            |
|                              | HP      | 2      | 0.05      | 0.1             |
| Pyro valves                  | NO      | 2      | 0.16      | 0.32            |
|                              | NC      | 5      | 0.145     | 0.725           |
| Check Valves                 |         | 2      | 0.085     | 0.17            |
| Propellant Filter            |         | 2      | 0.285     | 0.57            |

|                     |  |   |       |        |
|---------------------|--|---|-------|--------|
| He Filter           |  | 1 | 0.088 | 0.088  |
| Pipes & Interfaces  |  | 1 | 1.85  | 1.85   |
| Propellant tanks    |  | 4 | 2     | 8      |
| He tank             |  | 1 | 1.5   | 1.5    |
| Mass excl. Engines  |  |   |       | 15.663 |
| <b>Main Engines</b> |  |   |       |        |
| Type 1              |  | 4 | 0.77  | 3.08   |
| Type 2              |  | 4 | 0.68  | 2.72   |
| Type 3              |  | 4 | 0.56  | 2.24   |
| AT (HT)             |  | 2 | 0.275 | 0.55   |
| CGT(He)             |  | 2 | 0.03  | 0.06   |

### Safety Aspects of the Propulsion System

Investigation regarding safety aspects of the propulsion system have also been conducted using FMECA tools (reliability block diagrams, fault-trees...). The aim of a reliability study is to examine the way in which the spacecraft may fail in order to tailor the design and eliminate or limit failures to an acceptable level.

The FMECA worksheet form delineates the most plausible failures, their corresponding effects, their probabilities of occurrence, compensatory features, remarks and recommended corrective actions at the appropriate level. It contains :

- An enumeration of items or parts being analyzed
- A failure mode analysis which identifies the specific manner in which a part or system malfunctions. A failure mode is an “observed” or “external” effect.
- The determination of failure mode mechanism
- A description of the various effects of the failure mode on the next higher component level (Fault Tree Analysis).
- All the existing compensatory provisions which are already contained in the equipment or system to circumvent or

alleviate the effects of postulated failure mode.

- The effect on engine performance and on the mission
- The calculation of failure probability. This part defines a criticality index based on:
  - ♦ the probability that the failure occurs
  - ♦ the severity factor which describes the degree of reduced functionality resulting from the failure
  - ♦ the detectability factor of the failure
- A list of recommended corrective actions in case of malfunction

All possible ways of failure are examined in a systematic manner, and with a fault tree it is possible to see, for example, the different causes of a decreasing specific impulse and choose the best compensatory action. The fault-tree (example see figure 20) is used to establish consequences of a component failure on the system. The basic symbols used in a fault tree are shown in table 2.

Table 2: Fault Tree Basic Symbols

| Symbol  | Explanation   |
|---|---|
|  | “or” gate logic symbol . For a positive output one or more input must be positive |
|  | “and” gate logic symbol . For a positive output all input must be positive        |
|  | An event which results from a logic gate output                                   |

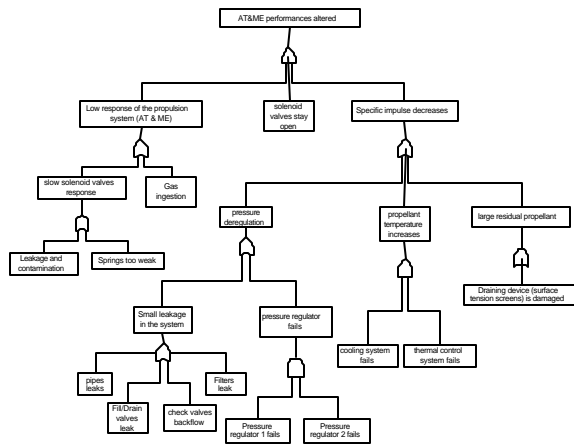


Figure. 20: Example of a Propulsion System Fault Tree during the Operational Phase

## Attitude Determination & Control System

The main task of the proposed microspacecraft ADCS is to determine and control the spacecraft attitude, i.e., to stabilize the spacecraft, and to orient it in the desired directions during the mission, despite the external and internal forces acting on it. Specifically, for the LunarSat mission the following tasks and analyses have been conducted during the course of the ADCS design:

- Operational ADCS modes have been identified.
- Impact of the environment on the ADCS have been described.
- Subsystem constraints have been identified.
- Hardware components and the subsystem architecture have been selected.
- Power and mass budgets have been provided.
- Interfaces with other subsystems and with the payload have been identified.
- Required ADCS algorithms and control strategies were identified.

- Implementation of determination and control algorithms is in progress.

Specifically, for LunarSat, due to the frequently required re-pointings, the complex mission goals, and the inertial characteristics of the spacecraft, a 3-axis stabilization technique has been selected for the LunarSat spacecraft. The ADCS hardware that is foreseen consists of:

- 4 Fiber optic laser gyros
- 1 Sun sensor
- 1 Star sensor
- 4 Solar Cells (Broad Sun sensor)
- 3 Reaction wheels
- 4 Attitude thrusters

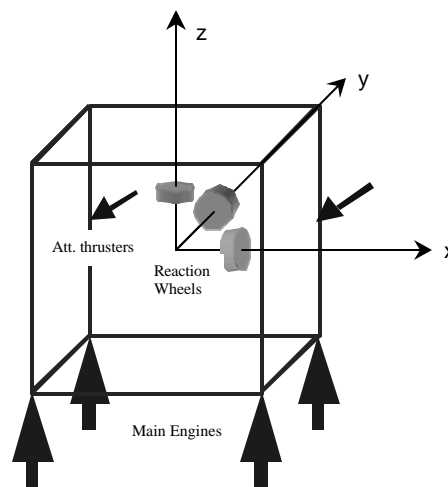


Figure22 : Baseline Actuators Layout of the LunarSat ADCS

### ADCS Modes

The ADCS modes identified for the LunarSat mission are:

- *Acquisition mode.*  
After Ariane 5 release the satellite will acquire its attitude, eventually stopping residual rotational movements
- *Parking mode.*

During GTO and Lunar Transfer Orbit phases, the satellite will point towards the Sun for power needs and will frequently point towards the Earth and the Moon with the camera

- **Firing mode.**  
During every orbital maneuver the spacecraft fires its 4 main engines and is controlled by off-pulsing them appropriately
- **Lunar orbit mode.**  
During this phase LunarSat will accomplish most of its mission tasks pointing the cameras towards the south pole of the Moon, pointing the high gain antenna towards Earth in order to send/receive data and pointing the solar cells toward the Sun.
- **Safe mode.**  
When a mishap takes place, the satellite has to keep its attitude and/or gain as much power as possible from the Sun.
- **Orbit maintenance mode.**  
In order to keep the Lunar orbit within nominal boundaries, some firings with the main engines will be required.

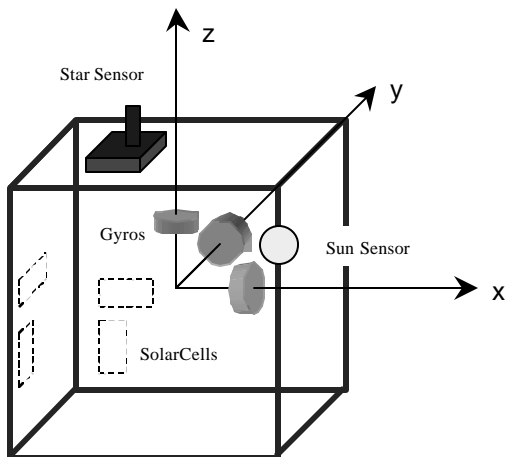
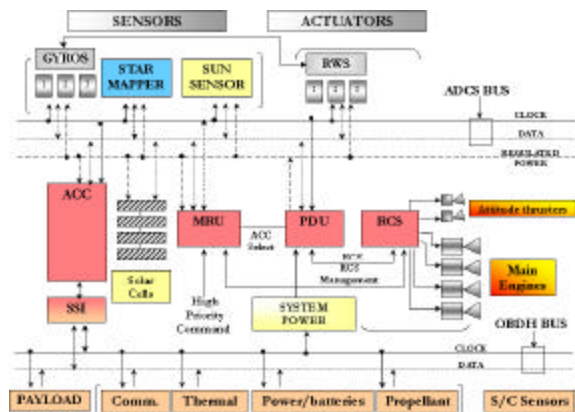


Figure 23: Baseline Sensors Layout of the LunarSat ADCS

### ADCS Requirements

The minimum requirements for the LunarSat ADCS are:

- Required Pointing Accuracies:
  - High gain Antenna Pointing:  $\pm 10^\circ$
  - Solar Panel Pointing:  $\pm 5^\circ$
  - Camera Pointing:  $\pm 0.2^\circ$
- Maximum jitter requirement:  $0.001^\circ$  in 100 ms
- Required Slew Speed (required for high resolution imaging during perilune passage):  $2^\circ/s$
- Requirement for availability of attitude data over the S/C bus: once a second
- Max. peak power consumption: 75 W



- ADCS SENSORS:**
- Gyros: 3 Laser Gyros LITEF
  - Star Mapper: KM 1301
  - Sun Sensor: DJO FSS
  - Solar Cells: 4 Backup Sun Sensors
- ADCS ACTUATORS:**
- RWS: Reaction Wheel System (3 RW: IRE)
  - RCS: Reaction Control System
    - 2 Attitude Thrusters (1N) Kayser Marquardt
    - 4 Main Engines (22N) Kayser Marquardt
- ADCS CONTROL:**
- ACC: Attitude Control Computer
    - Collection of Sensors's Data
    - Distribution of Actuators Commands
    - Attitude Determination
    - Mode control
  - SSI: SubSystem Interface
    - Acquisition of other subsystem data
  - MRU: Management and Reconfiguration Unit
    - Watchdog functions (Backup processor)
  - PDU: Power Distribution Unit
    - Distribution and switching of power
    - Selection of active ACC

Figure 21: Principle Layout of the Microspacecraft ADCS

### Control Strategy

The main characteristics regarding the LunarSat control strategy is that it is not designed for an Earth orbit mission. Therefore:

- It has to accomplish different main engine firings (increasing the difficulty of the mission)
- It has to accomplish tasks that are completely different (such as inertial pointings, imaging, etc).
- LunarSat will be launched with an ASAP (Ariane Structure for Auxiliary Payload), platform of the European Ariane 5, imposing an envelope constraint of 60 cm x 60 cm x 80 cm and a mass constraint of 100kg.
- LunarSat is a micro-satellite that implies it has a restricted mass budget. (It is not yet proven that micro-satellites can conduct interplanetary missions).

All these aspects drive the control of LunarSat spacecraft towards a 3 axis-stabilized solution. LunarSat has to accomplish several maneuvers in a relatively short time. *Three-axis control* permits stable and accurate maneuvers, depending on sensors and actuators. With respect to the selection of a 3-axis stabilization system for LunarSat, it needs to be mentioned that there is a trend towards this kind of stabilization, for all deep space probes and satellites. Table 3 provides an overview of past deep space missions, categorized in spin stabilized and 3-axis stabilized spacecrafts.

It is interesting to note that satellites with low resolution cameras in high orbits mostly use spin stabilization (e.g. MeteoSat, GMS, GEOS), while those with higher resolutions cameras (like LunarSat) use low orbits and 3-axis stabilization (e.g. NOAA, Meteor, LandSat, SPOT). Finally, it has to be added that micro-satellites with three-axis stabilization have already flown. Examples are LoSatX (1991) and TUBSAT B (1994). This is mainly due to the fact that technology succeeded in miniaturizing all those components that once could be flown only on big satellites. A spin stabilized technique was investigated for the orbital insertion phases of

LunarSat. However, due to the inertial characteristics of the spacecraft, the 3-axis stabilized solution was chosen.

Table 3: Past Deep Space Missions Attitude Control Strategies

| Spin stabilized   | 3-axis stabilized    |
|-------------------|----------------------|
| Pioneer 1-11      | Ranger 3-9           |
| Pioneer-Venus 1+2 | Lunar Orbiter 1-5    |
| Giotto            | Surveyor 1-5         |
| Lunar Prospector  | Luna 7-24            |
| Galileo           | Zond 3-8             |
|                   | Mariner 4-10         |
|                   | Mars 1-7             |
|                   | Venera 1-16          |
|                   | Vega 1+2             |
|                   | Viking 1+2           |
|                   | Voyager 1+2          |
|                   | Phobos 1+2           |
|                   | Phobos '96           |
|                   | Magellan             |
|                   | Ulysses              |
|                   | Cassini / Huygens    |
|                   | Mars Observer        |
|                   | Mars Pathfinder      |
|                   | Mars Global Surveyor |
|                   | Mars Polar Lander    |
|                   | Mars Climate Orbiter |
|                   | Deep Space I         |
|                   | NEAR                 |

### Control During Firings

One of the most critical phases for the ADCS is control during the orbital insertion firings. The inertial characteristics of the satellite change dramatically when propellant is consumed (this is easily understandable considering the fact that more than 40% of the initial mass of the satellite is propellant). Also, the position of the center of mass will change, due to the non-symmetrical configuration of the spacecraft structure. This shift of the center of mass will act as a disturbance torque that has to be counteracted. The dynamics of the system are relatively fast and make high control authority necessary.

During firing, the four main engines will accelerate the spacecraft and at the same time function as control actuators. By shutting off the appropriate thrusters for a short period of time (pulsing) the other thrusters will induce the necessary torque. Over time, this will provide the necessary thrust balance with respect to the position of the center of mass to keep the spacecraft attitude within the required limits.

For the sample time of the controller, different periods between 20 to 1000 ms have been tested. The concept of pulsing is as follows: For every time step the controller determines a shut-off time for two thrusters. If this time is less than 4 ms, which corresponds to the minimum impulse bit of the baseline thrusters, then no shut-off command will be given. Figure 22 shows the behavior of the spacecraft during the first of the foreseen LunarSat firings. The simulation sampling time is 1000ms. The graphs on the left show the LunarSat angular velocities. The second graphs on the right show the angular variations.

The increase in propellant consumption for control during insertion phases is caused by :

- Switching off the main engine thrusters leads us to a lower average level of thrust. Simulations show that instead of the original 88 N the average thrust level could drop down to 82 N. This causes a longer burning period and higher g-losses. These losses are translatable into an additional propellant mass requirement. According to the mission design, this quantity is on the order of 82 g for the GTO-LTO insertion and less than this quantity for LTO-LO insertion.
- By pulsing the main engines, we will have a need for more propellant because of a decrease of the nominal Isp of the thrusters (288 s). In order to roughly quantify the additional propellant needed, different

simulations have been conducted. From simulations it is possible to obtain a diagram of impulse width frequencies. using this diagram, the weighted average is calculated using the Isp vs. Impulse width chart (provided by the engines manufacturer). We obtained for the optimal controller simulation an Isp of 285.9 s, for the PID simulation an Isp of 285.34 s. It is possible, then, to relate the average Isp with the needed propellant for the foreseen 25 minutes of firing. This yields an additional propellant consumption of 340 g for optimal control simulation and 400 g for PID simulation.

- Small oscillations around the nominal direction also cause additional propellant consumption. This particular propellant consumption has been calculated as a percentage of the entire propellant consumed during firing phases. This percentage is 0.061% resulting in an additional  $\approx 20$  g of propellant.

### Control Algorithms

Different control algorithms have been developed and implemented using the Matlab/Simulink™ platform:

- *Detumble*
- *Control During Firing*
- *Inertial Pointing*
- *Spot Pointing*
- *Sun Pointing*

The firing phases algorithms require the main engines and the attitude thrusters as actuators. For inertial Sun, Earth and Moon pointings reaction wheels are used. Slewings are mainly accomplished with the reaction wheels. Also a master simulation model in Simulink which integrates all of the algorithms is being designed. It contains:

- Attitude dynamics and kinematics of the S/C,

- Models of the hardware used for the attitude determination and control (Thrusters, RW, Gyros, sun and star sensors),
- Controllers
- External and internal disturbances.
- It is easier to face the coupling terms that must be faced empirically with Classical PID Controllers,
- It is the most innovative and challenging solution for an „academic“ spacecraft like LunarSat

The use of this model will permit a complete simulation of the ADCS. The algorithms use internally quaternions to compute the attitude. A conversion from and to Euler angles is performed for input and output data. For every phase, two separate control algorithms are being developed:

- A PID controller based on classical control theory
- An optimal controller based on modern control theory

#### *Why PID control?*

The kind of controller which have been used in most of the spacecrafts is the PID controller, due to its simplicity and reliability. It is relatively easy to implement, and requires generally little performance of the on-board microprocessor.

#### *Why optimal control?*

Nowadays, thanks to a higher available computational power, it is not necessary anymore to regulate the dynamic of systems controlling only a few variables. The whole state of the dynamics system is controllable. An Optimal Controller minimizes a cost function that takes into account attitude requirement and maximum available power. This leads to many advantages:

- It is possible to set directly the angles and angular speeds accuracies and guarantee them to be small enough,
- It is the best mathematical solution for control multiple input and multiple output systems (control on 3-axes),

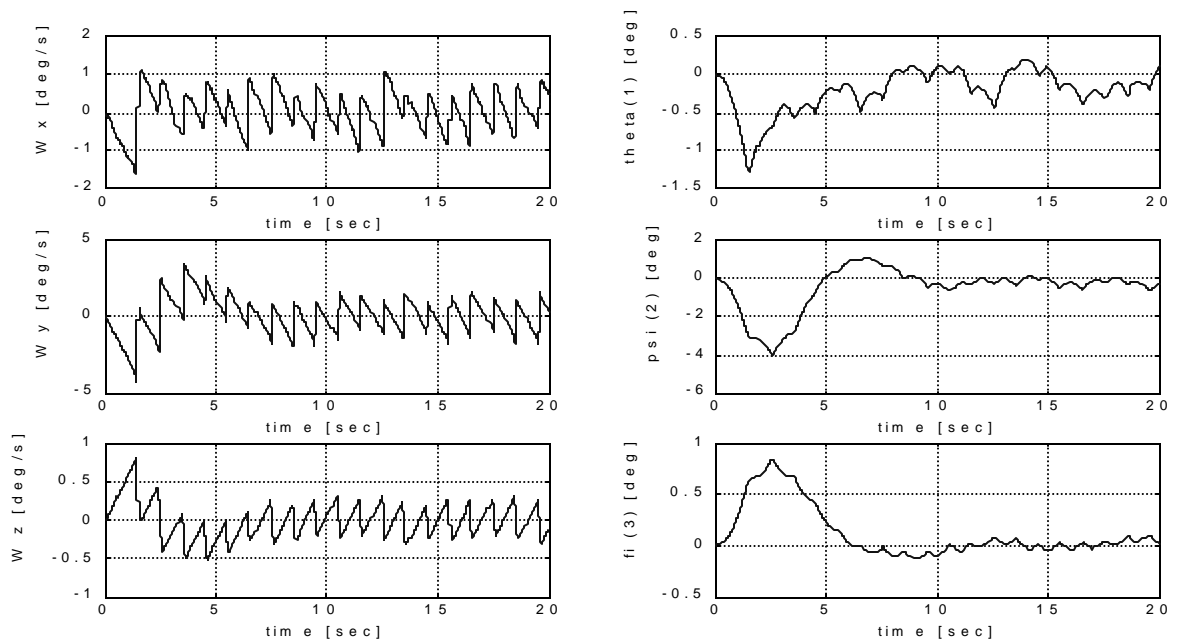


Figure 22: First Inertial Firing with 1000 ms Sampling Time

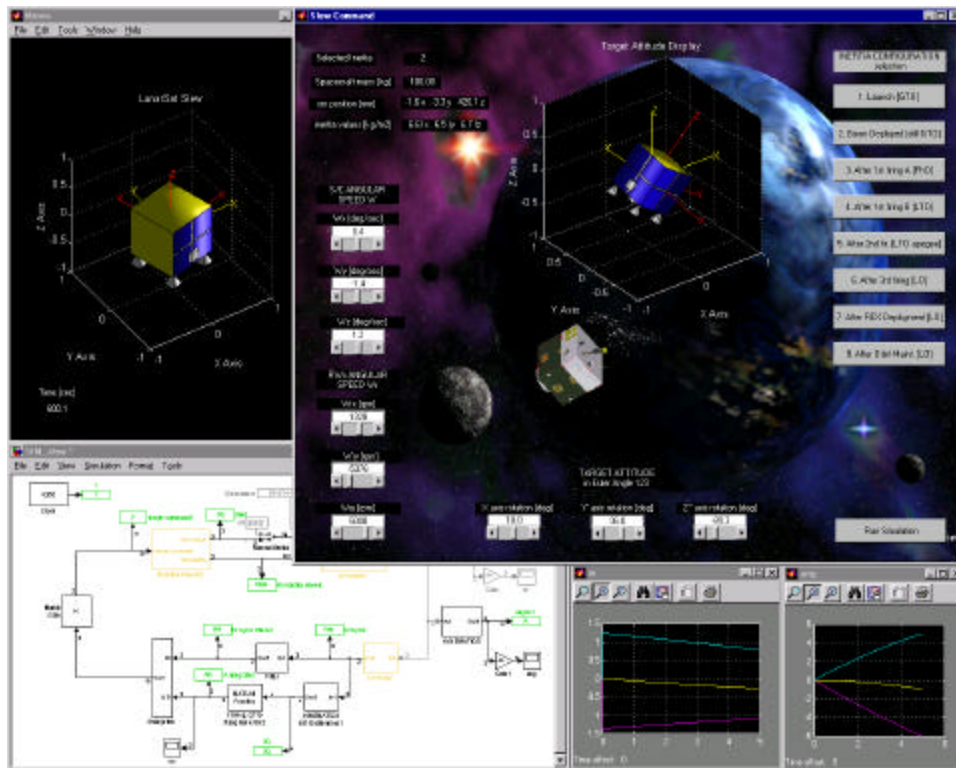


Figure 23: Some of the Implemented Matlab™ and Simulink™ Simulations

## Conclusions

The microspacecraft platform presented in this paper may be used to reach selected Earth orbits, the Lagrangian points of the Earth-Moon system, or lunar orbit and to achieve a Mars or Near-Earth object fly-by from GTO. The proposed design is based on the development of the LunarSat spacecraft and uses mainly COTS components. It thus provides a low-cost platform for certain exploration missions. It needs to be pointed out, however, that this type of spacecraft is significantly more expensive than a conventional microspacecraft due to the required propulsion system and the resulting increased complexity. Also, operations cost are typically much higher than for Earth orbiting missions. These aspects lead to the fact that a typical microspacecraft mission 'beyond LEO' may rather cost a few tens of million US-\$ instead of a few million US-\$, including launch, platform, payloads, and operations. Nevertheless, the designers of this concept strongly believe that the proposed platform concept will open up the door for future low-cost microspacecraft exploration missions.